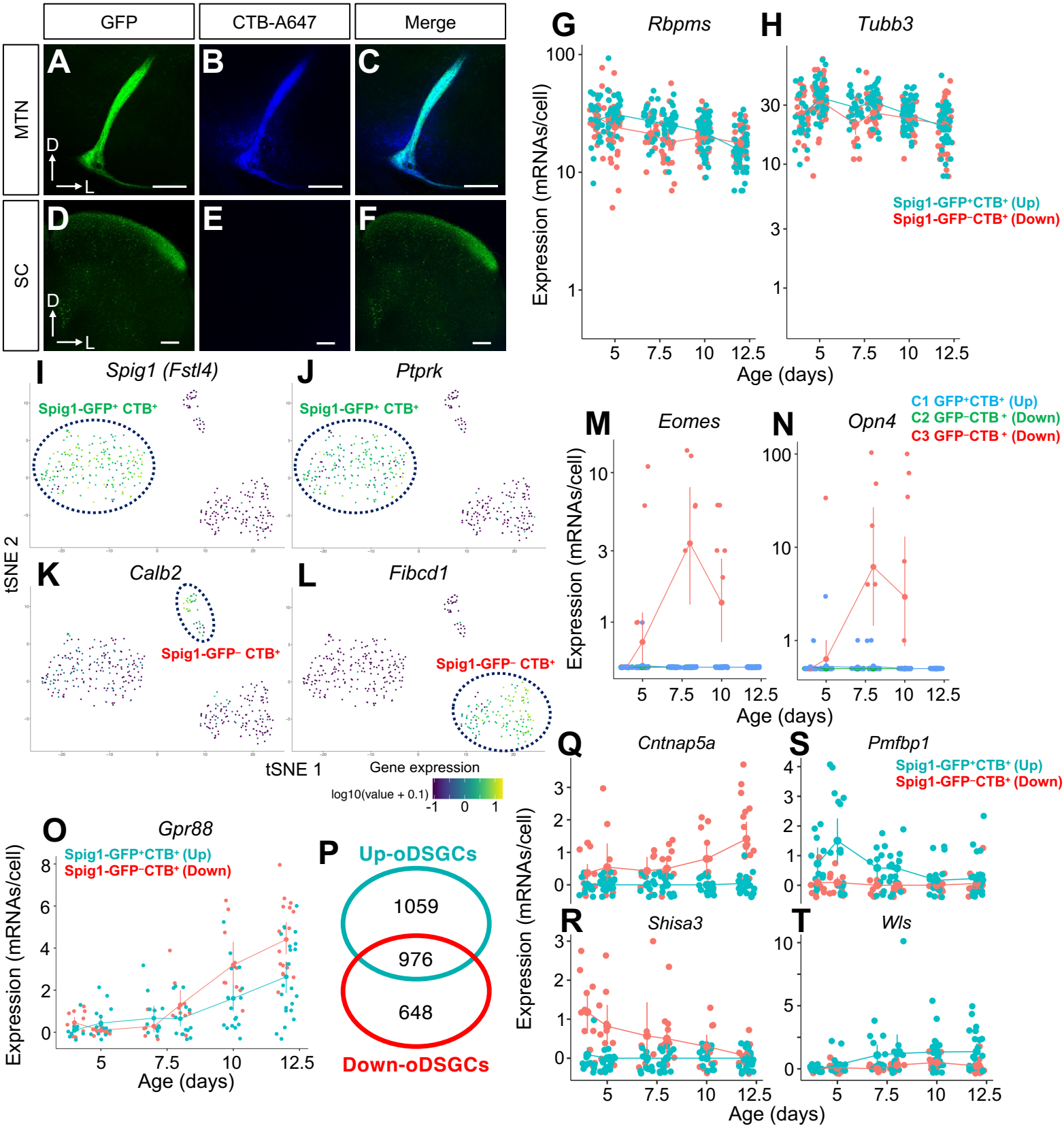
GFP
CTB-A647
Merge
MTN
SC
A
B
C
D
E
F
D
L
G
Rbpms
H
Tubb3
Expression (mRNAs/cell)
Age (days)
Spig1-GFP⁺CTB⁺ (Up)
Spig1-GFP⁻CTB⁺ (Down)
I
Spig1 (Fstl4)
J
Ptprk
Spig1-GFP⁺ CTB⁺
tSNE 2
tSNE 1
K
Calb2
L
Fibcd1
Spig1-GFP⁻ CTB⁺
Gene expression
log10(value + 0.1)
M
Eomes
N
Opn4
C1 GFP⁺CTB⁺ (Up)
C2 GFP⁻CTB⁺ (Down)
C3 GFP⁻CTB⁺ (Down)
O
Gpr88
P
Up-oDSGCs
1059
976
648
Down-oDSGCs
Q
Cntnap5a
S
Pmfbp1
R
Shisa3
T
Wls

Figure S1. Additional transcriptomic characterization of up- and down-oDSGCs, related to Figure 1.

(A-F) Coronal brain slices from P8 *Spig1-GFP* mice following CTB-A647 injection into the MTN at P3. After stereotactic injection of CTB-A647 into the MTN, brains from *Spig1-GFP* mice were examined to confirm the presence of CTB-A647 in the MTN (A-C) and the absence of CTB-A647 in other retinorecipient brain regions like the superior colliculus (SC) (D-F). **(G-H)** Single-cell RNAseq gene expression jitter plots show that both up-oDSGCs (Spig1-GFP^{+}CTB^{+}) and down-oDSGCs (Spig1-GFP$^{–}$CTB^{+}) express the RGC marker *Rbpms* (G) and the neuron marker *Tubb3* (H). Data presented as mean ± 95% confidence intervals. **(I-L)** tSNE plots show marker genes for the 3 populations of MTN-projecting DSGCs. *Spig1-GFP*$^{+}$ up-oDSGCs uniquely expressed *Spig1* (I) and *Ptprk* (J), the smaller cluster of *Spig1-GFP*$^{–}$ cells expressed *Calb2* (K), and the larger cluster of *Spig1-GFP*$^{–}$ cells expressed *Fibcd1* (L). **(M-N)** Single-cell RNAseq gene expression jitter plots showing the expression of *Eomes* (M) and *Opn4* (N), both markers of ipRGCs, in the small cluster of GFP$^{–}$CTB^{+} RGCs. Data presented as mean ± 95% confidence intervals. **(O)** In our single-cell RNAseq data, both up-oDSGCs and down-oDSGCs expressed *Gpr88*, a marker of up- and down-oDSGCs seen in the 10X Genomics single-cell RNAseq data from Tran and colleagues (2019). Data presented as mean ± 95% confidence intervals. **(P)** Venn diagram showing the number of genes that change between P4 and P12 in up- and down-oDSGCs. **(Q-T)** Exemplar genes that change linearly across time in down-oDSGCs (Q-R) and up-oDSGCs (S-T). Data presented as mean ± 95% confidence intervals. D, dorsal. L, lateral. Scale bars, 250 um.

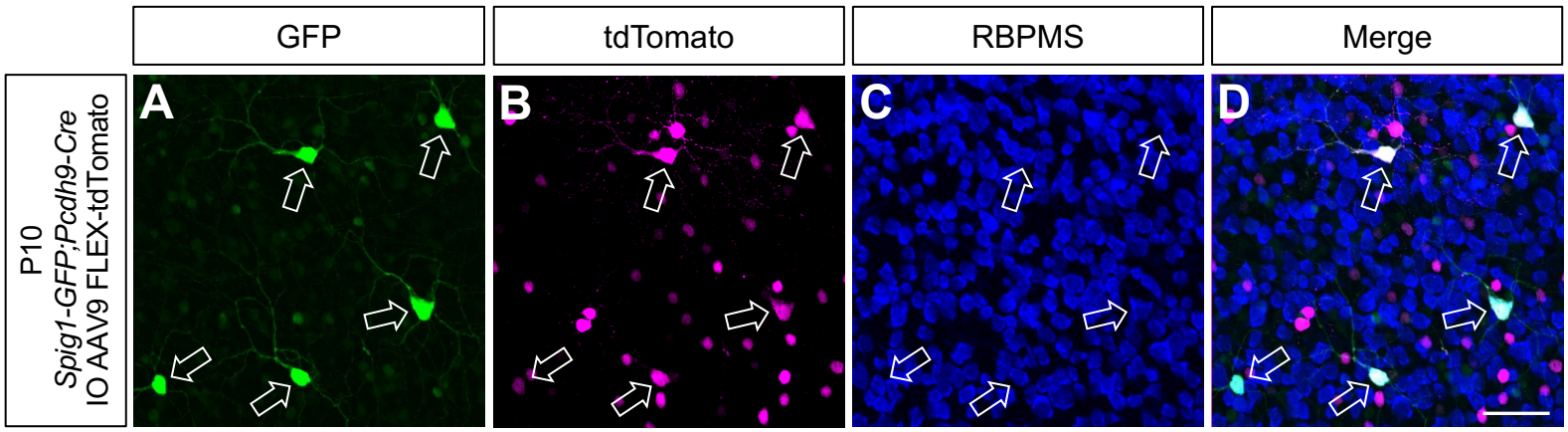

E

$$\frac{\text{GFP}^+\text{tdTomato}^+\text{RBPMS}^+}{\text{tdTomato}^+\text{RBPMS}^+} = \frac{74}{75} = 99\%$$

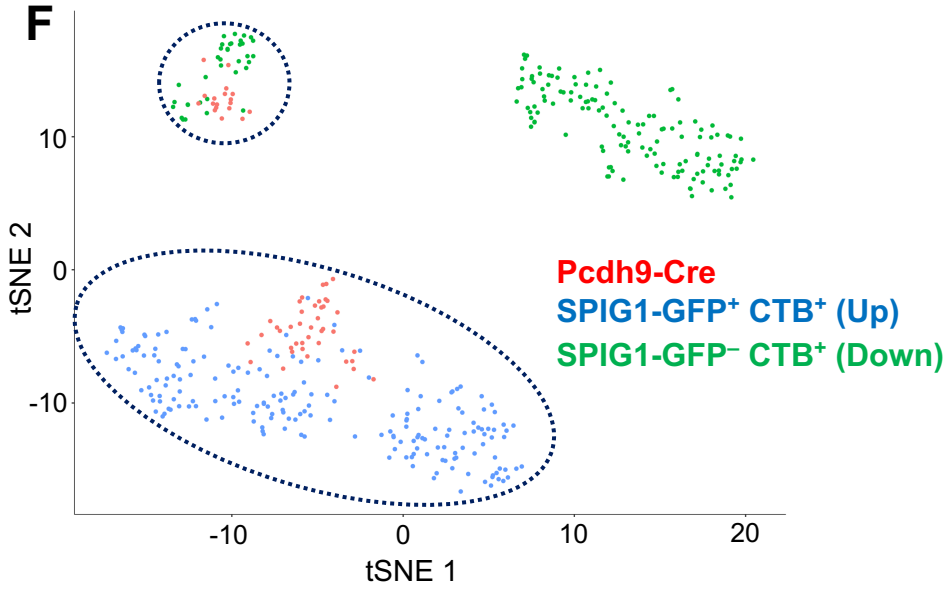

Figure S2. *Pcdh9-Cre* and *Spig1-GFP* both label up-oDSGCs, related to Figure 2.

(A-D) Whole-mount P10 *Pcdh9-Cre/+;Spig1-GFP/+* retina following an intraocular injection with AAV9 FLEX-tdTomato at P2 shows $GFP^+tdTomato^+RBPMS^+$ RGCs (arrows). **(E)** Among all $tdTomato^+$ *Pcdh9-Cre* RGCs, 99% were GFP^+. **(F)** Single-cell transcriptomes from P12 *Pcdh9-Cre* RGCs were combined with the existing single-cell transcriptomes from Spig1-GFP^+CTB^+ up-oDSGCs and Spig1-GFP^-CTB^+ down-oDSGCs between P4 and P12. The tSNE plot shows clustering of *Pcdh9-Cre* RGCs predominantly with *Spig1-GFP* RGCs. Scale bars, 50 um.

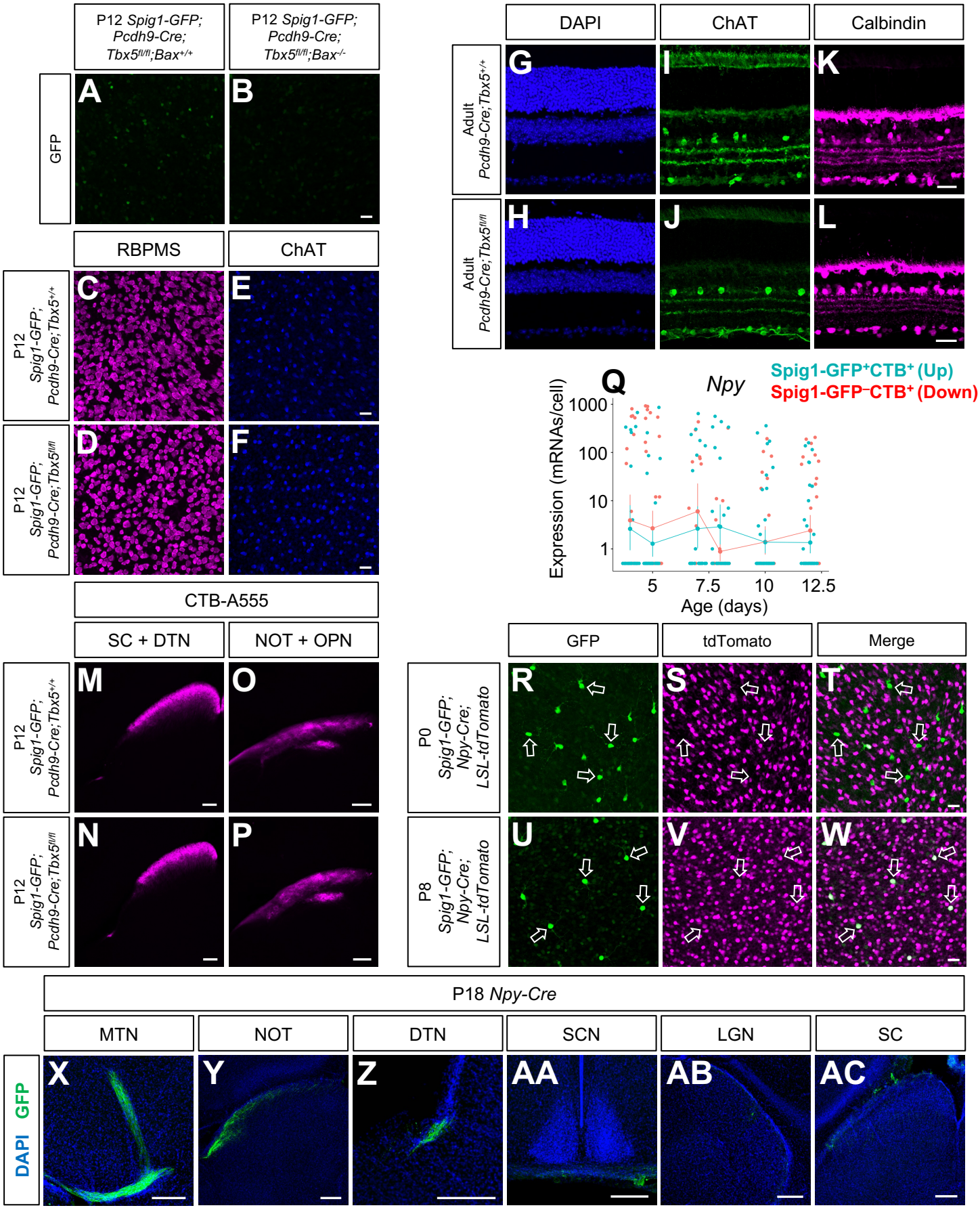
P12 Spig1-GFP; Pcdh9-Cre; Tbx5fl/fl;Bax+/+
P12 Spig1-GFP; Pcdh9-Cre; Tbx5fl/fl;Bax-/-
GFP
A
B
RBPMS
ChAT
P12 Spig1-GFP; Pcdh9-Cre;Tbx5+/+
P12 Spig1-GFP; Pcdh9-Cre;Tbx5fl/fl
C
E
D
F
DAPI
ChAT
Calbindin
Adult Pcdh9-Cre;Tbx5+/+
Adult Pcdh9-Cre;Tbx5fl/fl
G
I
K
H
J
L
Q
Npy
Spig1-GFP+CTB+ (Up)
Spig1-GFP−CTB+ (Down)
Expression (mRNAs/cell)
1000
100
10
1
5
7.5
10
12.5
Age (days)
CTB-A555
SC + DTN
NOT + OPN
P12 Spig1-GFP; Pcdh9-Cre;Tbx5+/+
P12 Spig1-GFP; Pcdh9-Cre;Tbx5fl/fl
M
O
N
P
GFP
tdTomato
Merge
P0 Spig1-GFP; Npy-Cre; LSL-tdTomato
P8 Spig1-GFP; Npy-Cre; LSL-tdTomato
R
S
T
U
V
W
P18 Npy-Cre
MTN
NOT
DTN
SCN
LGN
SC
DAPI GFP
X
Y
Z
AA
AB
AC

Figure S3. Additional phenotypic characterization of *Pcdh9-Cre;Tbx5$^{fl/fl}$* mice, related to Figure 3.

(A-B) At P12, Spig1-GFP^{+} up-oDSGCs were absent in both *Spig1-GFP;Pcdh9-Cre;Tbx5$^{fl/fl}$;Bax$^{+/+}$* and *Spig1-GFP;Pcdh9-Cre;Tbx5$^{fl/fl}$;Bax$^{-/-}$* retinas **(C-F)** RBPMS^{+} RGC density (C-D) and ChAT^{+} SAC density (E-F) were normal in P12 *Spig1-GFP;Pcdh9-Cre;Tbx5$^{fl/fl}$* retinas. **(G-L)** Gross retinal architecture, assessed by DAPI (G-H), and inner plexiform layer lamination, assessed by ChAT (I-J) and calbindin (K-L), were normal in adult *Pcdh9-Cre;Tbx5$^{fl/fl}$* retinas. **(M-P)** Innervation of the SC and DTN (M-N), as well as the NOT and OPN (O-P), was preserved in P12 *Spig1-GFP;Pcdh9-Cre;Tbx5$^{fl/fl}$* mice following intraocular injection with CTB-A555. **(Q)** Between P4-P12, both Spig1-GFP^{+}CTB^{+} up-oDSGCs and Spig1-GFP^{-}CTB^{+} down-oDSGCs expressed *Npy*, as measured by scRNAseq. Data presented as mean ± 95% confidence intervals. **(R-W)** GFP^{+} up-oDSGCs were tdTomato^{-} in *Spig1-GFP;Npy-Cre;LSL-tdTomato* mice at P0 (R-T), but became tdTomato^{+} by P8 (U-W). Arrows show example up-oDSGCs. **(X-AC)** P18 *Npy-Cre* mice showed innervation of the MTN, NOT, and DTN (X-Z), but not the SCN, LGN, or SC (AA-AC), following intraocular injection with AAV2 FLEX-GFP at P3. Scale bars, 25 um in (A-L) and (R-W); 250 um in (M-P) and (X-AC).

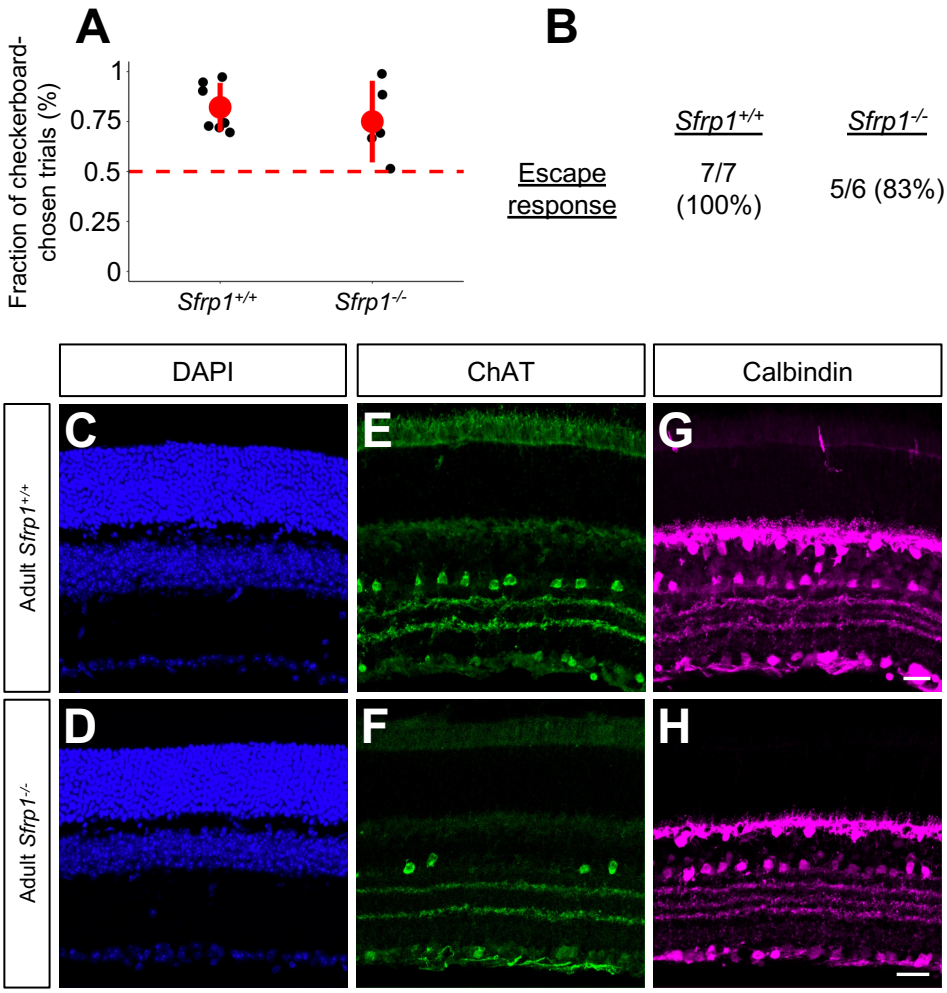
A
B
Fraction of checkerboard-chosen trials (%)
1
0.75
0.5
0.25
0
Sfrp1+/+
Sfrp1-/-
Sfrp1+/+
Sfrp1-/-
Escape response
7/7 (100%)
5/6 (83%)
DAPI
ChAT
Calbindin
Adult Sfrp1+/+
Adult Sfrp1-/-
C
D
E
F
G
H

Figure S4. Additional phenotypic characterization of *Sfrp1*$^{-/-}$ mice, related to Figure 4.

(A-B) Adult *Sfrp1*$^{-/-}$ mice showed intact depth perception on the visual cliff task (A) and intact escape behaviors on the looming task (B). Data presented as mean ± SD. **(C-H)** Gross retinal architecture, assessed by DAPI (C-D), and inner plexiform layer lamination, assessed by ChAT (E-F) and calbindin (G-H), were normal in adult *Sfrp1*$^{-/-}$ retinas. Scale bars, 25 um.